chemistry proceedings

MDPI

Proceeding Paper

Computational Survey of Two Specific Chalcone Derivatives to Study Their Structural, Electronic, and Chemical Behavior †

Rahul A. Shinde [1], Bhatu S. Desale [1], Tushar Janardan Pawar [2], Dipak B. Patil [2], Vishnu A. Adole [3,*] and Bapu S. Jagdale [3,*]

[1] Department of Chemistry, Mahatma Gandhi Vidyamandir´s Arts, Science and Commerce College, Manmad (Affiliated to Savitribai Phule Pune University, Pune), Nashik 423104, Maharashtra, India; rahulshinde843@gmail.com (R.A.S.); bhatudesale@rediffmail.com (B.S.D.)

[2] Departamento de Química, División de Ciencias Naturales y Exactas, Campus Guanajuato, Universidad de Guanajuato, Noria Alta S/N, Guanajuato 36050, Gto., Mexico tusharpawar49@gmail.com (T.J.P.); patildip98@gmail.com (D.B.P.)

[3] Department of Chemistry, Mahatma Gandhi Vidyamandir´s Loknete Vyankatrao Hiray Arts, Science and Commerce College, Panchavati (Affiliated to Savitribai Phule Pune University, Pune), Nashik 422003, Maharashtra, India

* Correspondence: vishnuadole86@gmail.com (V.A.A.); dr.jagdalebs@gmail.com (B.S.J.)

† Presented at the 26th International Electronic Conference on Synthetic Organic Chemistry; Available online: https://ecsoc-26.sciforum.net.

Abstract: Two previously reported 2,3-dihydro-1*H*-inden-1-one derived chalcone derivatives have been studied using density functional theory (DFT). This computational approach includes structural, electronic, physical, and chemical behavior of (*E*)-2-(thiophen-2-ylmethylene)-2,3-dihydro-1*H*-inden-1-one (TMDHI) and (*E*)-2-((1*H*-pyrrol-2-yl)methylene)-2,3-dihydro-1*H*-inden-1-one (PMDHI). The geometry of compounds was optimized by employing the DFT method with the B3LYP/6-311G (d,p) basis set. In this comparative study, various properties such as bond angle, bond length, dipole moment, augmentation in dipole moment, and total energy of TMDHI and PMDHI are revealed. Also, the study shows that the Mulliken atomic charges analysis revealed that all hydrogen atoms in both compounds have a positive charge and the molecular electrostatic surface potential plot of the title compounds showed negative potential located around the oxygen atom.

Keywords: DFT; Chalcone; TMDHI; PMDHI

Citation: Shinde, R.A.; Desale, B.S.; Pawar, T.J.; Patil, D.B.; Adole, V.A.; Jagdale, B.S. Computational Survey of Two Specific Chalcone Derivatives to Study Their Structural, Electronic, and Chemical Behavior. *Chem. Proc.* **2022**, *4*, x. https://doi.org/10.3390/xxxxx

Academic Editor(s): Julio A. Seijas

Published: 15 November 2022

1. Introduction

The chemistry of chalcones is one of the popular fields of organic synthesis. The exploration of Chalcones and related compounds always uncovers new methodologies and biological properties. Also, it has been found that chalcones acquired many applications in medicinal chemistry and biological science. [1–6] Furthermore, arylidene indanones, being one of the important chalcone skeletons commonly discovers surprising pharmacological applications due to the presence of α,β-unsaturated enone framework. [7–9] To comprehend the biological activity of chemical compounds, it is important to know their physical and chemical properties. Theoretical computations dependent on DFT have been effectively investigated to a great extent in the past couple of years to decide different various structural aspects of synthetically and pharmacologically vital organic motifs. [10–12] The density functional theory (DFT) inferred theoretical quantum calculations have been effectively utilized in many areas of science. DFT is a method that can generate a great deal of information about the physical and chemical behavior of various molecules. viet. [11–14] Cross-coupling reaction, equilibrium isotopic fractionation, pericyclic reaction, density-viscosity studies, catalysis, and photoelectronic applications are some

evident examples of DFT applications. [15–18] DFT calculations are useful for determining the structure and other important properties of molecules. DFT/B3LYP method utilizing different basis sets has been observed to be extremely crucial for researching chemical, electronic, thermodynamic and quantum chemical parameters. Also, bond lengths, bond angles, dipole moment, charge distribution, reactive sites, and other features could be investigated using the DFT method based on a computational study. The Computational study can be used to perform spectroscopic examinations such as IR, UV/Visible spectra, Raman, and NMR. In addition, DFT computations can also predict frontier molecular orbital energies and thereby the electronic excitation energy. [19–21] In continuation of our previous work and by considering these essential aspects, here we present a successful attempt to investigate structural parameters such as total energy, charge density, absolute electronegativity (χ), softness (σ), hardness (η), and electron transferred (ΔN), the electron density in highest occupied molecular orbital (HOMO) and lowest unoccupied molecular orbital (LUMO), of two previously synthesized arylidene indanones.

2. Methodology

2.1. Materials and Methods

The high-purity chemicals were purchased from a local distributor. The compounds were used exactly as they were received, with no further purification required. The melting point was investigated by the uncorrected open capillary. FT-IR spectra were obtained using potassium bromide pellets, while ^{1}H and ^{13}C NMR spectra were recorded with Bruker using $CDCl_3$ as the solvent. Thin-layer chromatography with aluminum sheets and silica gel 60 F254 was used to monitor the reaction (Merck).

2.2. Experimental Procedure for the Synthesis of TMDHI and PMDHI

The Claisen-Schmidt condensation reaction was used to synthesize the compounds TMDHI and PMDHI. In a typical synthesis method 2,3-dihydro-1*H*-inden-1-one (1, 10 mmol) and thiophene-2-carbaldehyde (2a, 10 mmol) or pyrrole-2-carbaldehyde (2b, 10 mmol) were combined in 10 mL ethyl alcohol. 5 mL 30% NaOH was added to this. The alkaline mixture was then stirred for 5-10 min at room temperature until the result formed. After the reaction was completed, it was poured onto crushed ice (as determined by TLC). It was then acidified with dilute HCl, filtered, dried, and recrystallized with hot ethanol to produce pure crystals of the products. The reaction is presented in Scheme 1.

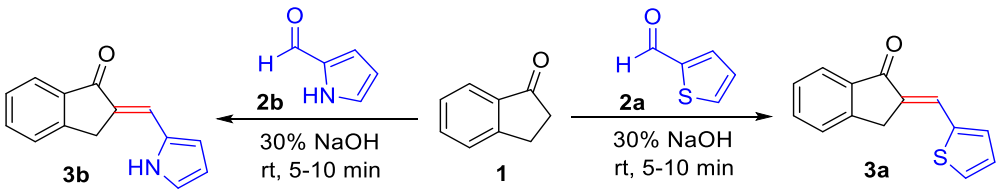

Scheme 1. Synthesis of the TMDHI and PMDHI.

2.3. Computational Details

Density Functional Theory (DFT) calculations were performed using the Gaussian-03 program package on an Intel (R) Core (TM) i5 computer with no geometry constraints. The DFT/B3LYP method was used to optimize the geometry of the title compounds using the 6-311G (d,p) basis set. The Guassview 4.1 molecular visualization program was used to create optimized geometry. The molecular electrostatic potential was computed using the same method to study the reactive sites of the title compounds. All the computations were done in the gas phase for the optimized structure. The DFT/B3LYP method with 6-311G (d,p) basis set was used to calculate Mulliken atomic charges.

3. Results and Discussion

3.1. Spectral Analysis of TMDHI and PMDHI

3.1.1. (*E*)-2-(Thiophen-2-ylmethylene)-2,3-dihydro-1H-inden-1-one (3a or TMDHI, $C_{14}H_{10}OS$)

Pale Yellow color; Yield 97%; m.p.: 122-124 °C; FT-IR (KBr, cm^{-1}): 3059.10, 2873.94, 1672.28, 1469.76 1415.75, 1371.39, 1251.80, 1201.65, 1099.43, 1029.99, 952.84, 908.47, 831.32, 781.17, 725.23, 663.51, 524.64, 472.56, 424.34, 358.76; ^{1}H NMR (500 MHz, $CDCl_3$) δ 3.97–3.93 (m, 2H), 7.18 (dd, *J* = 5.0, 3.7 Hz, 1H), 7.47–7.40 (m, 2H), 7.61–7.55 (m, 2H), 7.66–7.61 (m, 1H), 7.92–7.87 (m, 2H); ^{13}C NMR (126 MHz, $CDCl_3$) δ 193.89, 149.07, 139.92, 138.56, 134.58, 133.16, 132.76, 130.57, 128.23, 126.62, 127.69, 126.26, 124.34, 32.35.

3.1.2. (*E*)-2-((1*H*-pyrrol-2-yl)methylene)-2,3-dihydro-1*H*-inden-1-one (3b or PMDHI, $C_{14}H_{11}ON$)

Yellow color; Yield 85%; m.p.: 166-170 °C; FT-IR (KBr, cm^{-1}): 3059.10, 1668.43, 1597.06, 1415.75, 1369.46, 1317.38, 1247.94, 1201.65, 1107.14, 1068.56, 1026.13, 981.77, 908.47, 827.46, 779.24, 721.38, 663.51, 520.78, 470.63, 381.91; ^{1}H NMR (500 MHz, $CDCl_3$) δ 9.05 (s, 1H), 7.89 (ddd, *J* = 7.7, 1.3, 0.7 Hz, 1H), 7.67 (m, 1H), 7.63–7.53 (m, 2H), 7.47–7.39 (m, 1H), 7.08 (m, 1H), 6.76 (s, 1H), 6.46–6.40 (m, 1H), 3.92–3.88 (m, 2H); ^{13}C NMR (126 MHz, $CDCl_3$) δ 194.06, 148.87, 138.94, 134.14, 129.38, 129.25, 127.56, 126.11, 124.06, 123.66, 122.91, 114.89, 111.99, 32.37.

3.2. Computational Study

3.2.1. Molecular Structure, Bond Length, Bond Angle

Figure 1 shows the optimized molecular structure of the title compounds. Due to the overall asymmetry of the compounds, it is easy to see that both TMDHI and PMDHI have C1 point group symmetry from optimized molecular structures. Furthermore, the presence of a non-planar dihydrofuran ring in both compounds is evident. Dihydrofuran's non-planarity is due to the -CH_2- group (besides the oxygen atom), which is either above or below the plane. As a result, neither compound has a molecular plane (h). It can also be seen that the remaining skeletons of these compounds are in an ideal planar position, indicating that TMDHI and PMDHI have optimum geometrical structures. The optimized molecular geometry provides a good deal of information and therefore can have extended conjugation. This information is very much useful for the determination of various spectroscopic entities. The optimized geometrical parameters like bond lengths and bond angles of TMDHI and PMDHI are presented in Tables 1–4 respectively. The carbonyl bond length in TMDHI (C9-O14) and PMDHI (C1-O10) is 1.26 Å. The olefinic in both TMDHI (C10-C15) and PMDHI (C2-C11) is exactly the same 1.3552 Å. Other bond lengths are also in good agreement with the optimized structures. Bond angle data of both compounds are also in good agreement. PMDHI (4.97 Debye) appears to be more polar than TMDHI (4.28 Debye) based on the dipole moment data. The augmentation in the dipole moment in PMDHI is obviously due to the presence of a more electronegative nitrogen atom.

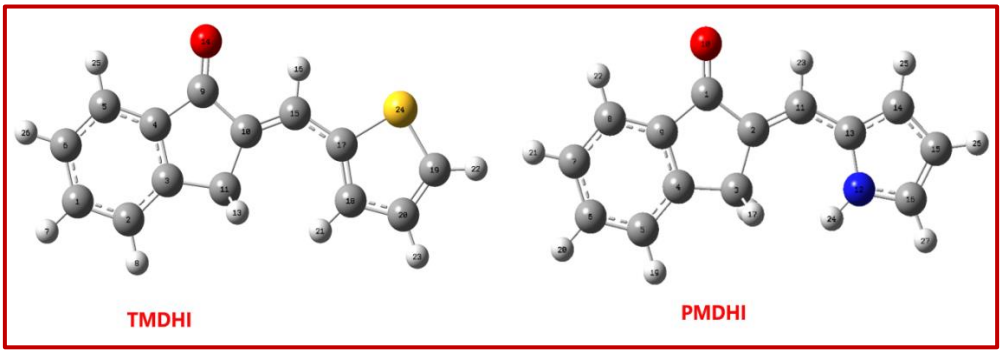

Figure 1. The optimized molecular structures of TMDHI and PMDHI at DFT B3LYP/6-311G(d,p) basis set.

Table 1. Optimized geometrical parameters of TMDHI by DFT/B3LYP with 6-311G (d,p) basis set.

Bond	Bond Length (Å)	Bond	Bond Length (Å)
C1-C2	1.4111	C10-C11	1.5425
C1-C6	1.4193	C10-C15	1.3552
C1-H7	1.0700	C11-C12	1.0700
C2-C3	1.3927	C11-H13	1.0700
C2-H8	1.0700	C15-H16	1.0700
C3-C4	1.3879	C15-C17	1.4014
C3-C11	1.5518	C17-C18	1.3642
C4-C5	1.3912	C17-S24	1.7639
C4-C9	1.5312	C18-C20	1.4240
C5-C6	1.4096	C18-H21	1.0700
C5-C25	1.0700	C19-C20	1.3642
C6-C26	1.0700	C19-H22	1.0700
C9-C10	1.5307	C19-S24	1.7639
C9-O14	1.2584	C20-H23	1.0700

Table 2. Optimized geometrical parameters of TMDHI by DFT/B3LYP with 6-311G(d,p) basis set.

Bond	Bond Angle (°)	Bond	Bond Angle (°)
C2-C1-C6	120.4723	C11-C10-C15	126.2943
C2-C1-H7	119.7632	C3-C11-C10	102.7679
C6-C1-H7	119.7642	C3-C11-H12	109.673
C1-C2-C3	118.0400	C3-C11-H13	113.0355
C1-C2-H8	120.9765	C10-C11-H12	109.5953
C3-C2-H8	120.9816	C10-C11-H13	113.1131
C2-C3-C4	121.0377	H12-C11-H13	108.5238
C2-C3-C11	127.4879	C10-C15-H16	120.0000
C4-C3-C11	111.4744	C10-C15-C17	120.0000
C3-C4-C5	121.9774	H16-C15-C17	120.0000
C3-C4-C9	109.4829	C15-C17-C18	124.7642
C5-C4-C9	128.5221	C15-C17-S24	124.7746
C4-C5-C6	117.7663	C18-C17-S24	110.4606
C4-C5-H25	121.1189	C17-C18-C20	113.5126
C6-C5-H25	121.1129	C17-C18-H21	123.2476
C1-C6-C5	120.3292	C20-C18-H21	123.2358
C1-C6-H26	119.8356	C20-C19-H22	124.7639
C5-C6-H26	119.8346	C20-C19-S24	110.4606
C4-C9-C10	105.8247	H22-C19-S24	124.7749
C4-C9-O14	127.0637	C18-C20-C19	113.5128
C10-C9-O14	127.0972	C18-C20-H23	123.2357
C9-C10-C11	107.4392	C19-C20-H23	123.2475
C9-C10-C15	126.2653	C17-S24-C19	90.8338

Table 3. Optimized geometrical parameters of PMDHI by DFT/B3LYP with 6-311G (d,p) basis set.

Bond	Bond length (Å)	Bond	Bond length (Å)
C1-C2	1.5272	C7-H21	1.0700
C1-C9	1.5327	C8-C9	1.5301
C1-O10	1.2584	C8-H22	1.0700
C2-C3	1.5392	C11-C13	1.5400
C2-C11	1.3552	C11-H23	1.0700
C3-C4	1.5534	N12-C13	1.4838
C3-H17	1.0700	N12-C16	1.4838
C3-H18	1.0700	N12-H24	1.0000
C4-C5	1.5315	C13-C14	1.3500
C4-C9	1.3464	C14-C15	1.5223

C5-C6	1.3646	C14-H25	1.0700
C5-H19	1.0700	C15-C16	1.3500
C6-C7	1.5575	C15-H26	1.0700
C6-H20	1.0700	C16-H27	1.0700
C7-C8	1.3633	-	-

Table 4. Optimized geometrical parameters of PMDHI by DFT/B3LYP with 6-311G (d,p) basis set.

Bond	Bond Angle (°)	Bond	Bond Angle (°)
C2-C1-C9	105.6284	C7-C8-C9	117.9669
C2-C1-O10	127.1953	C7-C8-H22	121.0126
C9-C1-O10	127.1619	C9-C8-H22	121.0186
C1-C2-C3	106.8042	C1-C9-C4	110.0000
C1-C2-C11	126.5817	C1-C9-C8	128.2495
C3-C2-C11	126.6127	C4-C9-C8	121.7324
C2-C3-C4	102.6254	C2-C11-C13	120.0000
C2-C3-H17	109.6314	C2-C11-H23	120.0000
C2-C3-H18	113.1576	C13-C11-H23	120.0000
C4-C3-H17	109.6918	C13-N12-C16	102.7785
C4-C3-H18	113.0973	C13-N12-H24	110.3561
H17-C3-H18	108.5029	C16-N12-H24	110.3556
C3-C4-C5	127.2496	C11-C13-N12	124.9617
C3-C4-C9	111.9489	C11-C13-C14	124.948
C5-C4-C9	120.8014	N12-C13-C14	110.0899
C4-C5-C6	118.2202	C13-C14-C15	107.1612
C4-C5-H19	120.8915	C13-C14-H25	126.4278
C6-C5-H19	120.8864	C15-C14-H25	126.4037
C5-C6-C7	120.5217	C14-C15-C16	107.1615
C5-C6-H20	119.7384	C14-C15-H26	126.4035
C7-C6-H20	119.7395	C16-C15-H26	126.4276
C6-C7-C8	120.3807	N12-C16-C15	110.0898
C6-C7-H21	119.8099	N12-C16-H27	124.9621
C8-C7-H21	119.8088	C15-C16-H27	124.9476

3.2.2. HOMO-LUMO and Reactivity Descriptor's Study

The highest occupied molecular orbital (HOMO) and lowest unoccupied orbital (LUMO) are collectively called frontier molecular orbitals (FMO). The FMO provides a lot of information about the stability and reactivity of molecules. Understanding several fundamental electronic aspects of the molecules requires an understanding of the energy gap between FMOs. TD-DFT/B3LYP method at 6-311G(d,p) basis set is used to obtain the HOMO-LUMO orbitals of the compounds under study. The HOMO-LUMO of TMDHI and PMDHI compounds are shown in Figure 2. The electronic parameters are given in Table 5. It is evident from the HOMO-LUMO energy data that the PMDHI compound has a more reactive HOMO and the TMDHI compound has a more reactive LUMO. Both ionization potential and electron affinity value of TMDHI are greater than PMDHI compound. The difference in energy gap value (ΔE) in TMDHI and PMDHI is negligible (Table 5). Also, the TMDHI compound has a slightly more inevitable charge transfer phenomenon which is validated by the charge transfer value (ΔN_{max} in Table 6). Using Koopman's theorem [22], various global reactivity parameters such as chemical hardness (η), chemical softness (σ), global electrophilicity (ω), electronegativity (χ), and chemical potential (μ) have been calculated from HOMO-LUMO energy values. The chemical hardness and softness values suggest that both compounds are polarizable. The TMDHI compound has more electrophilicity index as compared to PMDHI.

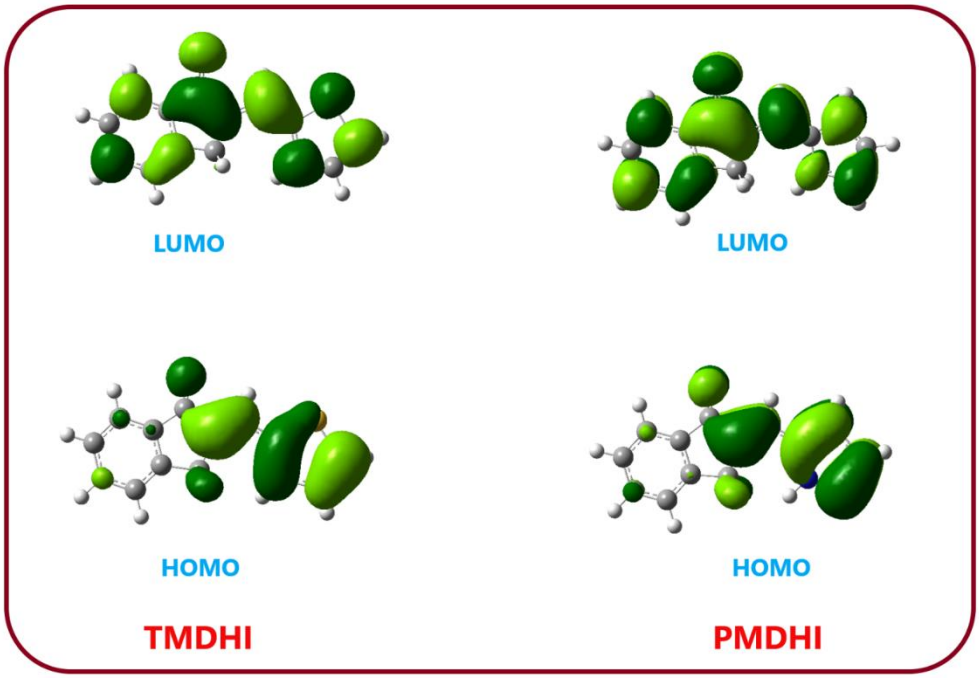

Figure 2. HOMO-LUMO representation of TMDHI and PMDHI at TD-DFT B3LYP/6-311G(d,p) basis set.

Table 5. Electronic parameters.

Electronic Parameters	TMDHI	PMDHI
E_{Total} (a.u.)	−1013.08	−670.25
E_{HOMO} (eV)	−6.23	−5.81
E_{LUMO} (eV)	−2.40	−2.12
I (eV)	6.23	5.81
A (eV)	2.40	2.12
ΔE (eV)	3.83	3.69

Table 6. Global reactivity parameters.

Global Reactivity Parameters	TMDHI	PMDHI
η (eV)	1.91	1.84
σ (eV^{-1})	0.52	0.54
ω (eV)	4.95	4.26
X (eV)	4.35	3.96
μ (eV)	− 4.35	− 3.96
ΔN_{max} (eV)	2.28	2.15

3.2.3. Mulliken Atomic Charges and MESP Analysis TMDHI and PMDHI

The Mulliken population analysis [23] gives rise to Mulliken's charges. It explains how to use computational simulations to calculate partial atomic charges. Mulliken's charges are those that are based on charge density. Tables 7 and 8 show the Mulliken atomic charges of TMDHI and PMDHI, respectively. The graphical presentation of Mulliken´s atomic charges in Figure 3 revealed that all hydrogen atoms in both compounds have a positive charge. The most negative and positive carbon atoms in TMDHI, according to Mulliken's population analysis, are C17 (-0.289104) and C9 (0.229276), respectively. On the other hand, C2 (−0.212715) and C1 (0.233053) are the most negative and positive carbon atoms in PMDHI. Also, Figure 4 characterizes the Molecular Electrostatic Surface

Potential plot *(MESP)* and Contour plot of TMDHI and PMDHI. MESP correlates a molecule's total charge distribution with its dipole moment, electronegativity, partial charges, and chemical reactivity site which provides a visual technique for understanding a molecule's relative polarity and can be used to illustrate hydrogen bonding, reactivity, and the structure-activity relationship. It's a proton's potential energy at a specific position near a molecule. Different colors correspond to different values of the electrostatic potential at a molecule's surface. In general, locations with attracting potential are red, whereas those with repulsive potential appear blue. In the title compounds, the negative potential is located around oxygen atoms.

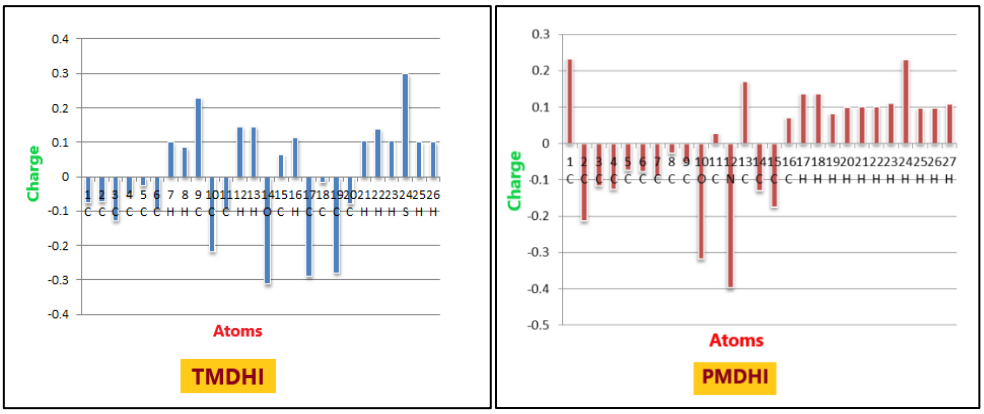

Figure 3. Graphical representations of Mulliken atomic charges of TMDHI and PMDHI.

Table 7. Mulliken atomic charges of TMDHI.

Atom	Charge	Atom	Charge
1 C	−0.076750	14 O	−0.311977
2 C	−0.072450	15 C	0.064495
3 C	−0.126599	16 H	0.112672
4 C	−0.050045	17 C	−0.289104
5 C	−0.025596	18 C	−0.017300
6 C	−0.090894	19 C	−0.279449
7 H	0.100220	20 C	−0.078322
8 H	0.084509	21 H	0.104101
9 C	0.229276	22 H	0.136900
10 C	−0.217264	23 H	0.104287
11 C	−0.091529	24 S	0.297920
12 H	0.145453	25 H	0.101314
13 H	0.145448	26 H	0.100684

Table 8. Mulliken atomic charges of PMDHI.

Atom	Charge	Atom	Charge
1 C	0.233053	15 C	−0.174635
2 C	−0.212715	16 C	0.071373
3 C	−0.117113	17 H	0.137003
4 C	−0.125741	18 H	0.137010
5 C	−0.074563	19 H	0.081793
6 C	−0.078164	20 H	0.098929
7 C	−0.090555	21 H	0.099950
8 C	−0.027462	22 H	0.100748
9 C	−0.050736	23 H	0.109267

10	O	−0.318016	24	H	0.230848
11	C	0.027235	25	H	0.096810
12	N	−0.397939	26	H	0.096999
13	C	0.169697	27	H	0.107705
14	C	−0.130779	-		-

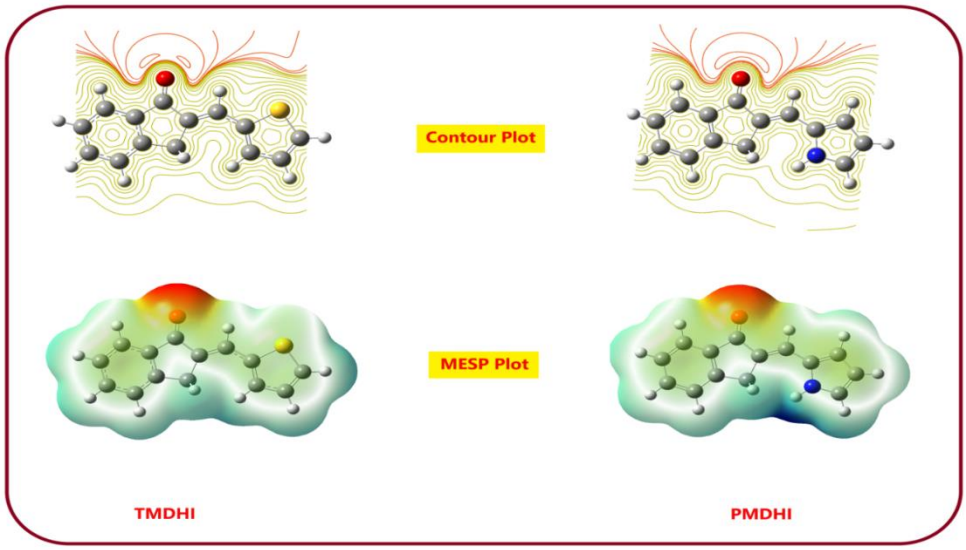

Figure 4. Molecular electrostatic surface potential plot (MESP) and Contour plot of TMDHI and PMDHI.

4. Conclusions

In conclusion, we have studied two chalcone derivatives of 2,3-dihydro-1H-inden-1-one: (E)-2-(thiophen-2-ylmethylene)-2,3-dihydro-1H-inden-1-one (TMDHI) and (E)-2-((1H-pyrrol-2-yl)methylene)-2,3-dihydro-1H-inden-1-one (PMDHI). Using DFT at B3LYP/6-311G(d,p) basis package, a detailed structural study has been performed by exact molecular structure, bond length, and bond angle. Both compounds have C1 point group symmetry, meaning that the compounds are overall asymmetric. The unavoidable charge transfer phenomenon occurs in both compounds. The carbonyl bond length in TMDHI (C9-O14) and PMDHI (C1-O10) is nearly 1.26 Å. The olefinic in both TMDHI (C10-C15) and PMDHI (C2-C11) is exactly the same which is 1.3552 Å. Other bond lengths are also in agreement with the optimized structures. Bond angle data of both compounds are also in good agreement. PMDHI (4.97 Debye) appears to be more polar than TMDHI (4.28 Debye) based on the dipole moment data. The augmentation in the dipole moment in PMDHI is obviously due to the presence of a more electronegative nitrogen atom. The total energy of TMDHI is less than PMDHI compound suggesting that TMDHI compound is less reactive and more stable. The Mulliken's atomic charges analysis revealed that all hydrogen atoms in both compounds have a positive charge. The Mulliken's atomic charges analysis revealed that all hydrogen atoms in both compounds have a positive charge. The most negative and positive carbon atoms in TMDHI, according to Mulliken's population analysis, are C17 (−0.289104) and C9 (0.229276), respectively. On the other hand, C2 (−0.212715) and C1 (0.233053) are the most negative and positive carbon atoms in PMDHI.

Acknowledgments: The Authors acknowledge the central instrumentation facility (CIF), Savitribai Phule Pune University, Pune for the spectral analysis and CIC, KTHM College, Nashik for FT-IR spectral analysis. The authors are also grateful to A. B. Sawant for the Gaussian study. Aapoorva P. Hiray, Coordinator of M. G. Vidyamandir institute is gratefully acknowledged for the Gaussian package.

References

1. Davison, E.K.; Brimble, M.A. Natural product derived privileged scaffolds in drug discovery. *Curr. Opin. Chem. Biol.* **2019**, *52*, 1–8.
2. Kar Mahapatra, D.; Asati, V.; Bharti, S.K. An updated patent review of therapeutic applications of chalcone derivatives (2014-present). *Expert Opin. Ther. Pat.* **2019**, *29*, 385–406.
3. Lin, Y.; Qiu, D.; Huang, L.; Zhang, S.; Song, C.; Wang, B.; Wu, J.; Chen, C. A novel chalcone derivative, L2H17, ameliorates lipopolysaccharide-induced acute lung injury via upregulating HO-1 activity. *Int. Immunopharmacol.* **2019**, *71*, 100–108.
4. Zhuang, C.; Zhang, W.; Sheng, C.; Zhang, W.; Xing, C.; Miao, Z. Chalcone: A privileged structure in medicinal chemistry. *Chem. Rev.* **2017**, *117*, 7762–7810.
5. Xu, M.; Wu, P.; Shen, F.; Ji, J.; Rakesh, K.P. Chalcone derivatives and their antibacterial activities: Current development. *Bioorganic Chem.* **2019**, *91*, 103113.
6. Ouyang, Y.; Li, J.; Chen, X.; Fu, X.; Sun, S.; Wu, Q. Chalcone Derivatives: Role in Anticancer Therapy. *Biomolecules*, **2021**, *11*, 894.
7. Adole, V.A.; Pawar, T.B.; Jagdale, B.S. Aqua-mediated rapid and benign synthesis of 1, 2, 6, 7-tetrahydro-8H-indeno [5, 4-b] furan-8-one-appended novel 2-arylidene indanones of pharmacological interest at ambient temperature. *J. Chin. Chem. Soc.* **2020**, *67*, 306–315.
8. Adole, V.A.; Bagul, V.R.; Ahire, S.A.; Pawar, R.K.; Yelmame, G.B.; Bukane, A.R. Computational chemistry: molecular structure, spectroscopic (UV-visible and IR), electronic, chemical and thermochemical analysis of 3′-phenyl-1, 2-dihydrospiro [indeno [5, 4-b] furan-7, 2′-oxiran]-8 (6h)-one. *J. Adv. Sci. Res.* **2021**, *12*, 276–286.
9. Elkanzi, N.A.; Hrichi, H.; Alolayan, R.A.; Derafa, W.; Zahou, F.M.; Bakr, R.B. "Synthesis of Chalcones Derivatives and Their Biological Activities: A Review. *ACS Omega* **2022**, *7*, 27769–27786.
10. Kapil, J.; Shukla, P.; Pathak, A. Density Functional Theory. *Recent Trends Mater. Devices* **2020**, *256*, 211–220.
11. Adole, V.A. Computational Chemistry Approach for the Investigation of Structural, Electronic, Chemical and Quantum Chemical Facets of Twelve Biginelli Adducts. *J. Appl. Organomet. Chem.* **2021**, *1*, 29–40.
12. Zhao, T.; Liu, Q.L.; Zhao, Z.Y. High-throughput screening delafossite $CuMO_2$ (M= IIIA, 3d, 4d, 5d, and RE) optoelectronic functional materials based on first-principles calculations. *J. Phys. Chem. C* **2019**, *123*, 14292–14302.
13. Shinde, R.A.; Adole, V.A.; Jagdale, B.S. Antimicrobial and computational investigation of two 2, 3-dihydro-1 H-inden-1-one derived fluorinated chalcone motifs. *Vietnam. J. Chem.* **2021** *59*, 800–812.
14. Pracht, P.; Grant, D.F.; Grimme, S. Comprehensive Assessment of GFN Tight-Binding and Composite Density Functional Theory Methods for Calculating Gas-Phase Infrared Spectra. *J. Chem. Theory Comput.* **2020**, *16*, 7044–7060.
15. Adole, V.A.; Waghchaure, R.H.; Pathade, S.S.; Patil, M.R.; Pawar, T.B.; Jagdale, B.S. Solvent-free grindstone synthesis of four new (E)-7-(arylidene)-indanones and their structural, spectroscopic and quantum chemical study: a comprehensive theoretical and experimental exploration. *Mol. Simul.* **2020**, *46*, 1045–1054.
16. Iron, M.A.; Gropp, J. Cost-effective density functional theory (DFT) calculations of equilibrium isotopic fractionation in large organic molecules. *Phys. Chem. Chem. Phys.* **2019**, *21*, 17555–17570.
17. Akerling, Z.R.; Norton, J.E.; Houk, K.N. DFT study of pericyclic reaction cascades in the synthesis of antibiotic TAN-1085. *Org Lett.* **2004**, 6, 4273–4275
18. Weijing, D.; Weihong, Z.; Xiaodong, Z. The application of DFT in catalysis and adsorption reaction system. *Energy Procedia*. **2018**, *152*, 997–1002.
19. Noureddine, O.; Gatfaoui, S.; Brandan, S.A.; Sagaama, A.; Marouani, H.; Issaoui, N. Experimental and DFT studies on the molecular structure, spectroscopic properties, and molecular docking of 4-phenylpiperazine-1-ium dihydrogen phosphate. *J. Mol. Struct.* **2020**, *1207*, 127762.
20. Suresh, S.; Gunasekaran, S.; Srinivasan, S. Spectroscopic (FT-IR, FT-Raman, NMR and UV–Visible) and quantum chemical studies of molecular geometry, Frontier molecular orbital, NLO, NBO and thermodynamic properties of salicylic acid. Spectrochim. *Acta A Mol. Biomol. Spectrosc. Spectrochim. Acta A* **2014**, *132*, 130–141.
21. Dhonnar, S.L.; Adole, V.A.; Sadgir, N.V.; Jagdale, B.S. Structural, Spectroscopic (UV-Vis and IR), Electronic and Chemical Reactivity Studies of (3, 5-Diphenyl-4, 5-dihydro-1H-pyrazol-1-yl)(phenyl) methanone. *Phys. Chem. Res.* **2021**, *9*, 193–209.
22. Koopmans, T. Uber die Zuordnung von Wellenfunktionen und Eigenwerten zu den einzelnen Elektronen eines atoms. *Physica*. **1934**, *1*, 104–113.
23. Mulliken, R.S. Electronic Population Analysis on LCAO-MO Molecular Wave Functions. *Int. J. Chem. Phys.* **1955**, *23*, 1833–1840.